NIGERIAN JOURNAL OF ENVIRONMENT AND HEALTH
Elucidating the Environment-Health Nexus in Nigeria
ISSN: 2616-0714 (print edition) eISSN: 2616-0706 (online, open access)

Nigerian Journal of Environment and Health 3 (2020) 19–28

Performance Evaluation of Rainfall Models and Associated Precipitation Oscillations in the Southwestern Climate System of Nigeria

A. A. Willoughby[a], A. O. Ndubuisi[b], O. F. Dairo[a,c,*], A. O. Soge[a]

[a]*Department of Physical Sciences, Redeemer's University, P. M. B. 230, Ede, Osun State 232102, NIGERIA*
[b]*Department of Physics, Covenant University, Ota, Ogun State, NIGERIA*
[c]*Department of Electrical and Electronic Engineering, Redeemer's University, P. M. B. 230, Ede, Osun State 232102, NIGERIA*

Abstract

The study explored the spatio-temporal evolution of rainfall and precipitable water oscillations using data of over two decades. The monthly averages of rainfall and precipitable water were obtained from six locations in the southwestern climatic region of Nigeria. The data were analysed using five mathematical models namely the sum of two-Gaussians, the sum of two-Lorentzian, Fourier on four harmonics, sine wave and fourth-order polynomial functions for prediction purposes. The performances of these models were evaluated using the mean bias error (MBE), root mean square error (RMSE), mean percentage error (MPE), standard error (SE) and the correlation coefficient (R). The performance indicators of the models showed that the Gaussian and Lorentzian models are in good agreement with the observed data. However, the Fourier on fourth harmonics model had the lowest MBE, RMSE and MPE, consequently highest correlation coefficient values, indicating high model accuracy. Thus, the Fourier model has the best correlation with the observed data and is recommended for estimating these variables in the selected locations.

© NJEH 2020 Published by Living Science Foundation.

Keywords: Rainfall pattern, annual variation, predictive models, precipitable water, statistical test.

1. Introduction

Scientific observation and modelling of rainfall and precipitable water are essential to meet the sustainable development goals (SDGs) of Climate Action (13), Zero Hunger (2), No Poverty (1), Clean Water and Sanitation (6). SDG 13, in particular, strengthens resilience and adaptive capacity of nations to climate-related hazards and natural disasters, which ensure the fulfilment of SDGs 1, 2 and 6. Analysing the data obtained will improve education and increase awareness on these SDGs. The derived statistics will be integrated into mitigation, adaptation, impact reduction, or early warning policies and strategies to plan and implement national development in various sectors. These sectors may range from geographical, agricultural, remote sensing, to urban and regional planning.

Similarly, the data find application in satellite and terrestrial radio propagation and water and environmental engineering. Environmental and water reticulation software, commercial farm management software products, and many others require diurnal and seasonal predicted or recorded data obtained from the mathematical implementation of

Accepted 20 August 2021.
*Corresponding author
Email address: dairof@run.edu.ng (O. F. Dairo)

modelling functions. Radio propagation models use radio refractivity estimates derived from pressure, temperature, and relative humidity. Energy software and thermal heating systems require approximations of solar radiation and temperature resource observed at the location where the system is to be installed. Of all the six meteorological variables under consideration, solar radiation is considered dominant in determining the spatial-temporal variations of the other variables. Many studies have been investigated to obtain empirical models for the estimation of solar irradiance and other meteorological parameters at the earth's surface in Nigeria. These models have been developed from records of databases archived by meteorological weather stations in different regions of the country. A majority of these predictive models are based on existing empirical models proposed and developed by individual researchers.

2. Research Objectives

In this research, five mathematical models namely sum of two-Gaussians, sum of two-Lorentzians, Fourier on fourth harmonic (depicted as Fourier FH in the plots), sine wave, and 4th order polynomial functions were considered. They were used to estimate the monthly average data points of solar radiation, temperature, precipitable water, sunshine hours, rainfall, and relative humidity for six cities in the Southwest zone of Nigeria. The outcome is a set of monthly-predicted meteorological data as a function of the observed data input. The deviations of the predicted data from the observed were then assessed using standard error analysis to test the accuracy of the function. The performance accuracy of these models was validated using mean bias error (MBE), root mean square error (RMSE), and mean percentage error (MPE) to determine the best fit for the variables.

3. Precipitable Water

Precipitable water is an essential atmospheric variable for climate system calculation (Ortiz de Galisteo et al., 2011). It is the depth of water in a column of the atmosphere expressed in the height to which the water substance would reach if condensed and collected in a vessel. Precipitable water has a considerable effect on solar radiation, especially in humid regions (Li et al., 2014). It is a good indicator of how much rain or snow might fall due to a thunderstorm or a low-pressure system. The concept of precipitable water has applications in different areas such as precipitation forecast, remote sensing (Oduro-Afriye, 1992), and atmospheric transmission spectrum (Maduekwe and Ogunmola, 1997; Udoh and Okujagu, 2014).

4. Rainfall

Akinbobola et al. (2018) worked on the statistical modelling of monthly rainfall in fourteen selected stations in Nigeria's rain forest and savannah eco-climatic regions. Their study concluded that Seasonal Autoregressive Integrated Moving Average (SARIMA) model was a proper method for modelling and predicting the monthly rainfall. The results help forecast the pattern of rainfall in the study area. Ekwe et al. (2014) examined the mathematical study of monthly and annual rainfall patterns in Nasarawa State for 20 years (1993-2012) using data obtained from the archives of Meteorological Observatory at the College of Agriculture, Lafia, Nasarawa State, Nigeria. Statistical techniques like time series analysis, mean and standard deviation were employed to depict the temporal distribution of rainfall over the area. Analysing the months under consideration, it was noticed that August recorded the highest rainfall value of 2498 mm, which is the month where clouds pervade the sky.

5. Seasonal trends of the meteorological parameters in the study area

The southwest region of Nigeria comprising the stations under study is characterised by two distinct seasons: the rainy season, beginning in April and ending in October, and the dry season characterised by the Harmattan, a dry dust-laden atmosphere blown down by the northeast trade winds. It descends south from the Sahara desert into the sub-region in November and retreats in March. The seasonal patterns of the parameters as observed in the mean monthly values might be directly associated with and controlled by the annual migration of the Inter-Tropical Discontinuity (ITD), also known as Inter-Tropical Convergence Zone (ITCZ). The ITD is the north-south oscillation of a zone of discontinuity between the moist, south-westerly, tropical maritime (mT) monsoon air mass originating

from the Gulf of Guinea and the cool dry, north-easterly tropical continental (cT) wind blowing in from the Sahara desert (Dairo and Kolawole, 2018; Willoughby et al., 2002; Ojo, 1970; Adejokun, 1966). The ITD follows the sun so that its location varies seasonally, consequently responsible for dry and wet seasons in the tropics. It forms a low-pressure belt near the equator where the northeast and southwest trade winds converge, thus generating severe convective activity such as thunderstorms. The movement and fluctuations of this phenomenon dictate and control the solar radiation, rainfall, and water vapour profiles characteristic of the country (Dairo and Kolawole, 2018; Ogolo and Adeyemi, 2009; Willoughby et al., 2002). The migration of the ITD reaches its maximum northward extent in July/August and its maximum southward summit in January (Ojo, 1970). At the beginning of the wet season, the ITD holds an approximate position between 10° N and 12° N, and during this time, it has migrated far north, exposing southern Nigeria to the wet season. In May/June, it moves further northward to 15° N - 16° N such that widespread rainfall is experienced over areas south of 10° N (Olaniran, 1988). A slight drop in mean values of the meteorological parameters during the wet months is usually observed in August. This reduced mean value observed for precipitable water, temperature, and relative humidity is coincidental with the temporary rainfall reduction. This short-term diminution of the rate and amount of daily rainfall is commonly referred to as the "Little Dry Season", (LDS) (Adejuwon and Odekunle, 2006). During this August 'drought' or 'break', which lasts for about two to three weeks, stations under the influence of wet season exhibit double rainfall maxima with peaks at about May/June and September/October. The phenomenon is characteristic of the West African equatorial region, between geographical 4° N and 9° N, and 7° E and 12° W, wherein lie the southwest of Nigeria (Ilesanmi, 1981; Adefolalu, 1972; Adekoya, 1979; Omotosho, 1988). This occurs when the ITD line is at its northmost position (Balogun, 1981). In January, the position of the ITD moves to approximately 9° N, and all regions north of this latitude will be under the influence of the dry cT air mass, resulting in dry season conditions. The six stations come under the dry season spell resulting in a significant reduction in rainfall, water vapour, humidity and precipitable water values.

6. Methods

6.1. Data Acquisition

Twenty-one years averaged datasets (1981-2012) obtained from Nigerian Meteorological agency (NIMET) were used in the model assessment. Figure 1 shows the geographical location of each of the stations in the southwest region of Nigeria. The average of these parameters was computed and used in the mathematical models.

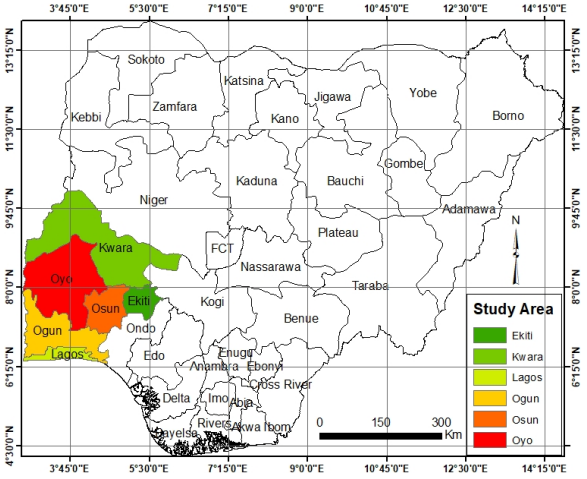


Figure 1. Map showing southwest region study area.

6.2. Prediction Models

Curve fitting models are mathematical functions that provide the best mathematical description or fit a set of data points. The function returns a set of estimated data based on observed or experimental data. For the model

Table 1. Geographical coordinates of the stations under consideration.

S/N	Stations	Coordinates	
		Lat	Lon
1	Abeokuta (Ogun)	7°9′ N	3 °21′ E
2	Ado-Ekiti (Ekiti)	7°37′ N	5 °13′ E
3	Ibadan (Oyo)	7°22′ N	3 °54′ E
4	Ikeja (Lagos)	6°35′ N	3 °20′ E
5	Ilorin (Kwara)	8°30′ N	4 °32′ E
6	Osogbo (Osun)	7°46′ N	4 °34′ E

to be appreciably accurate, the deviations from the observed data points must be negligible. A measure of deviation commonly used to test the exactness of the model is the minimum RMSE. Four model functions were applied to assess which best fits the observed data to model the variables that appear to be exhibiting periodic variations. Gaussian, Lorentzian, Fourier, sine, and polynomial functions, with their corresponding yield in coefficients, were utilised in this work. Gaussian and Lorentzian non-linear regression functions are the most widely used for fitting bell-shaped curves with peaks, although the Lorentzian has a more expansive 'tail' spread. However, due to the seasonal double maxima exhibited by rainfall, precipitable water and relative humidity, the sum of two-Gaussians and sum of two-Lorentzians functions were deemed more suitable for the curve fitting than the standard single Gaussian or Lorentzian distributions (Willoughbya et al., 2019).

7. Results and Discussion

Figures 2 - 3 show that rainfall and precipitable water exhibit two peaks, one in June and the other in September, with a trough in August. The mid-year dip indicates a reduction in the average monthly values, usually between June and September.

7.1. Precipitable Water

Figures 2(a)-(f), which illustrate the comparison between the modelled and observed precipitable water data for Abeokuta, Ado-Ekiti, Ibadan, Ikeja, Ilorin, and Osogbo, show that precipitable water has two peaks in each of the cities. In Abeokuta, the first peak is observed in June while the second in late August with a dip between July and early August. In Ado-Ekiti, the two peaks are marked in early June and September with a dip in August. Similarly, two peaks are seen in Ibadan and Ikeja, between May and June, and between August and September. In Ilorin, the peaks are observed in June and September. The first peak in Osogbo is evident between May and June while the second peak is in September, with a dip between July and August. The dip between the two peaks indicates a short duration of marked reduction in precipitable water between the two peaks. The variations in the rainfall peaks with months of the year are because of the geographical locations of each of the cities. Precipitable water, which is an indicator of the probable amount of rain, indicates a possibility of high amount of rainfall during the peaks. The dip, which is present in the observed data curve, is also present in the data curves of the other models except for the sine and polynomial models. However, it is observed that the Fourier model exhibits a better fit than the Gaussian and Lorentzian models. The sine and polynomial models largely deviate; hence, they depict poor accuracies of the modelled precipitable water data. Table 2 shows that the Fourier model has ideal performance indicators (MBE, RMSE, MPE) for precipitable water, with the lowest standard error for each city and the highest correlation coefficient of value 1. This indicates a perfect fit for the observed data of precipitable water. The sine model has the highest standard error values ranging from 0.97 in Ikeja to 0.64 in Osogbo, except Ilorin, where the polynomial model has a SE value of 0.76. Also, it has high underestimations for MBE and MPE. Polynomial model has negative values of MBE in each city, depicting severe underestimation, but gives an overestimation (positive MBE value) in Osogbo.

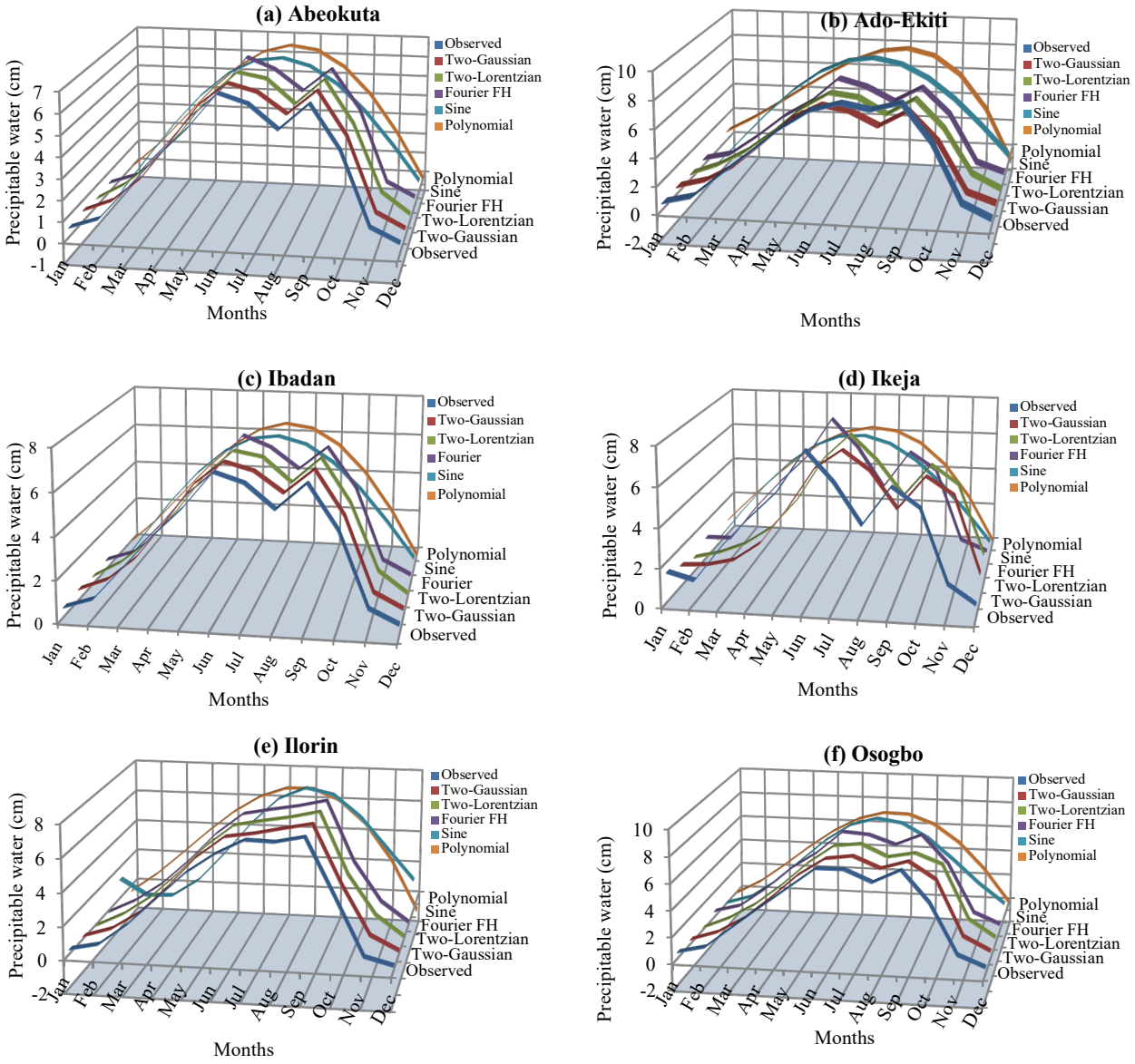


Figure 2. (a)-(f) Observed and modelled total precipitable water for the stations.

7.2. *Rainfall*

The observed and estimated Rainfall data are represented for each city in Figures 3(a)-(f). The variation curves depict two rainfall peaks. The first maximum occurs in June and the second occurs in September (after the LDS). This period is marked by low humidity and low temperature. The Fourier FH model curve shows the two peaks with the dip in between. It gives the best variation curve but slightly deviates in January and December. The curves of the two-Gaussians and two-Lorentzians models do not show a distinct dip as noted in the observed rainfall variation curve. The figures for the sine and polynomial models are without dips, suggesting that they are poor fits for the rainfall data. As observed in Table 3, the Fourier FH model has the least RMSE value while the polynomial model gives high RMSE values for each of the locations. This evaluation is also verified in the MBE values in which the fourth-order polynomial has the highest underestimation for each location. R is observed to hold the highest value for Fourier model. This suggests that Fourier model is suitable for the prediction of rainfall in these cities.

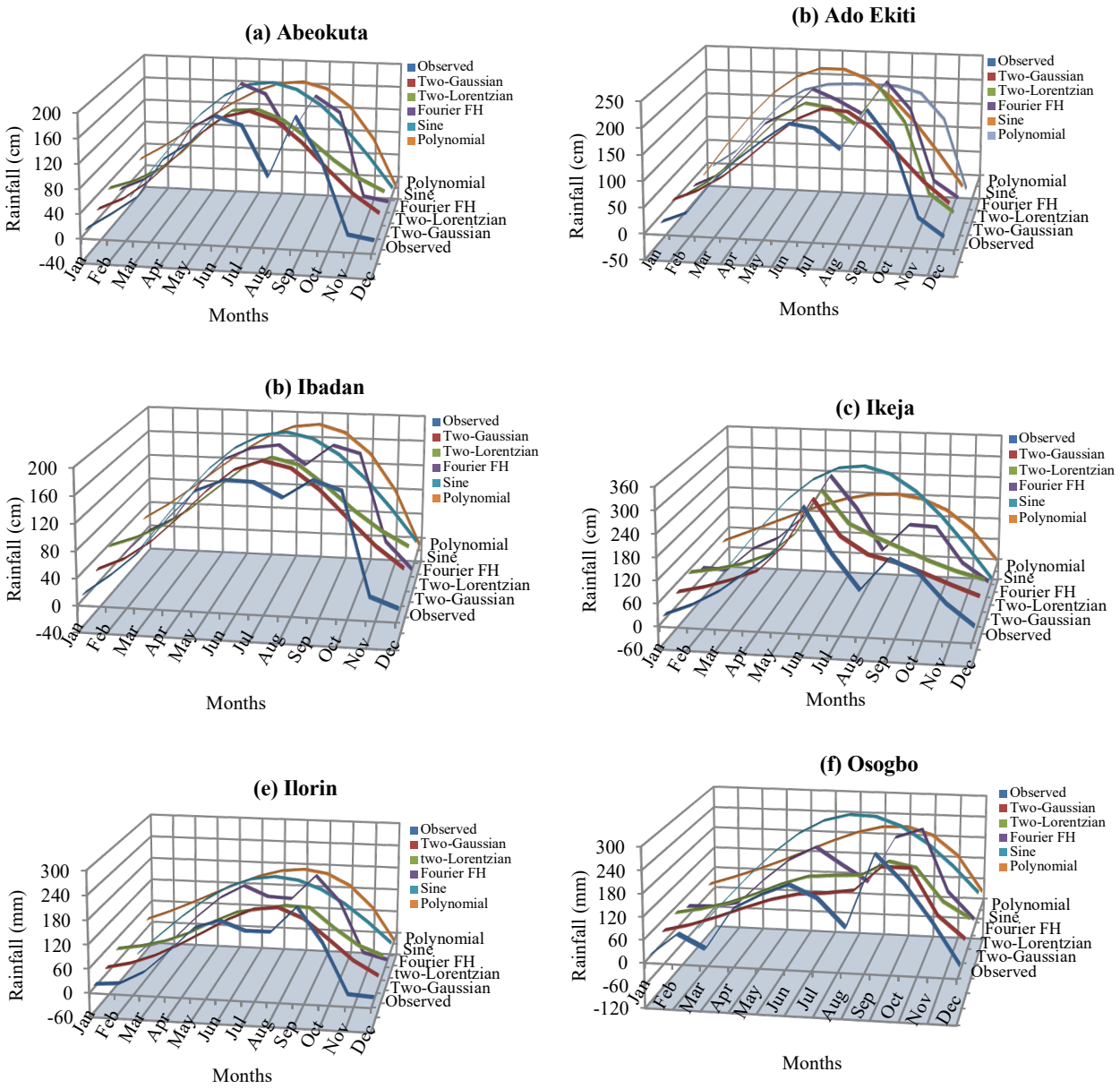


Figure 3. (a)-(f) Observed and modelled rainfall for the stations.

7.3. Statistical Test Results

The performance of each model was assessed statistically by computing the mean bias error (MBE), root mean square (RMSE) and mean percentage error (MPE). The standard error (SE) for each model is also presented. For accurate estimation, low values of MBE, RMSE, MPE, SE values, and a correlation coefficient R-value close to 1 are desired. Table 4 presents the performance indicators of the models for precipitable water in each location. It is observed that for Abeokuta, Fourier FH has the lowest MBE, RMSE and MPE (%). It has the lowest standard error and highest correlation coefficient R of 0.05 and 1.00, respectively. This is followed by the sum of two-Gaussians and sum of two-Lorentzians models, which have SE of 0.18. The sine wave has the highest SE and lowest R of 0.74 and 0.06, respectively. Fourier FH has the lowest MBE, RMSE, MPE (%) and SE across the six cities investigated, which indicate the best fit with the observed data. The statistical results are presented in Tables 4, showing a summary

of the performance indicators for the models of precipitable water and rainfall in each city. Also, Fourier FH has a correlation coefficient, R, of approximately 1.00 across all the cities. Figures 2-3 show that the estimated values of the models exhibit a good variation trend along with the observed data except the fourth-order polynomial model, which shows a poor agreement with the observed values. Table 4 summarises the results of the statistical indicators for the performance level of each of the models for both precipitable water and rainfall in the selected locations. Figures 2 and 3 show an increase in rainfall and precipitable water distributions during the rainy season and sustained decrease during the dry season. Also, for each location shown in Figures 2-3, the Fourier model gives a very good correlation, except in January and December. The other models do not fit the observed data well; particularly, the sine and polynomial models exhibit the poorest curve.

Table 2. Regression coefficients for Precipitable water at all the stations

PRECIPITABLE WATER

Location	Models	Regression Coefficients									
		a	b	c	d	g	h	k			
Abeokuta	Sum of two Gaussians	0.25	6.62	6.25	2.06	4.33	9.41	0.72			
	Sum of two Lorentzians	1.86	8.57	6.28	3.10	6.54	0.50	0.50			
	Sine wave	0.23	6.22	1.49	10.67	-	-	-			
	4th order Polynomial	-0.70	0.29	0.44	-0.06	0.00	-	-			
	Fourier 4 Harmonics	a	b	c_1	c_2	c_3	c_4	d_1	d_2	d_3	d_4
		4.01	.57	-2.1	-2.3	-.08	-.69	-.5	-.4	-.3	.3
Ado-Ekiti	Sum of two Gaussians	0.11	7.6	6.46	2.21	4.51	9.29	0.86			
	Sum of two Lorentzians	-3.39	10.87	6.49	3.74	4.81	9.34	0.82			
	Sine wave	0.49	7.34	1.69	10.45	-	-	-			
	4th order Polynomial	-0.19	0.72	0.15	0.01	-9E-04	-	-			
	Fourier 4 Harmonics	a	b	c_1	c_2	c_3	c_4	d_1	d_2	d_3	d_4
		4.8	0.57	-2.20	-3.10	-0.42	-.78	-.42	-.26	-.25	.15
Ibadan	Sum of two Gaussians	0.25	6.62	6.25	2.06	4.33	9.41	0.72			
	Sum of two Lorentzians	-1.86	8.58	6.28	3.1	6.53	9.44	0.49			
	Sine wave	0.25	6.25	1.50	10.70	-	-	-			
	4th order Polynomial	-0.69	0.29	0.44	-0.06	0.00	-	-			
	Fourier 4 Harmonics	a	b	c_1	c_2	c_3	c_4	d_1	d_2	d_3	d_4
		4.0	0.57	-2.0	-2.3	-0.1	-0.7	-0.5	-0.4	-0.3	0.3
Ikeja	Sum of two Gaussians	1.08	6.22	5.99	1.72	5.26	9.51	0.61			
	Sum of two Lorentzians	-0.16	7.58	5.97	2.17	9.25	9.49	0.41			
	Sine wave	0.44	6.00	1.10	11.17	-	-	-			
	4th order Polynomial	-0.56	1.29	0.05	-0.01	1E-04	-	-			
	Fourier 4 Harmonics	a	b	c_1	c_2	c_3	c_4	d_1	d_2	d_3	d_4
		4.2	0.57	-2.0	-1.9	0.44	-0.76	-0.59	-0.73	-0.39	-0.45
Ilorin	Sum of two Gaussians	-0.15	6.89	6.55	2.21	3.92	9.07	0.84			
	Sum of two Lorentzians	-2.61	8.56	6.3	3.33	4.99	8.93	1.11			
	Sine wave	3.86	3.74	4.31	5.73	-	-	-			
	4th order Polynomial	-1.13	0.43	0.35	-0.04	0.008	-	-			
	Fourier 4 Harmonics	a	b	c_1	c_2	c_3	c_4	d_1	d_2	d_3	d_4
		4.0	0.57	-2.1	-3.0	-0.60	-0.50	-0.46	-0.01	-0.23	0.19
Osogbo	Sum of two Gaussians	-0.14	7.42	6.59	2.42	3.94	9.44	0.56			
	Sum of two Lorentzians	-2.59	9.76	6.44	3.48	6.31	9.44	0.49			
	Sine wave	3.81	3.73	3.86	6.36	-	-	-			
	4th order Polynomial	-0.4	-0.04	0.55	-0.07	0.002	-	-			
	Fourier 4 Harmonics	a	b	c_1	c_2	c_3	c_4	d_1	d_2	d_3	d_4
		4.36	.57	-2.1	-2.7	-.2	-.72	-.48	-.37	-.28	-.25

Table 3. Regression coefficients for rainfall at all the stations

RAINFALL

Location	Models	Regression Coefficients									
		a	b	c	d	g	h	k			
Abeokuta	Sum of two Gaussians	-1.12	96.99	6.01	2.59	100	7.63	2.57			
	Sum of two Lorentzians	7.76	103.6	5.74	2.43	106.1	7.94	3.06			
	Sine wave	3.91	191.6	0.56	12.55	-	-	-			
	4th order Polynomial	3.72	17.39	2.85	-0.16	-0.02	-	-			
	Fourier on 4 Harmonics	a	b	c_1	c_2	c_3	c_4	d_1	d_2	d_3	d_4
		108.4	.57	-59.5	-58.1	2.1	-26.6	-22.8	-19.0	-20.8	13.0
Ado-Ekiti	Sum of two Gaussians	7.73	116.7	6.1	2.79	115.3	8.2	2.3			
	Sum of two Lorentzians	1.6	122.7	5.8	2.9	127.7	8.6	2.3			
	Sine wave	10.97	230.3	0.99	11.02						
	4th order Polynomial	11.38	20.6	2.03	-0.29						
	Fourier on 4 Harmonics	a	b	c_1	c_2	c_3	c_4	d_1	d_2	d_3	d_4
		136.0	.57	-56.2	-74.9	-4.8	-37.7	-18.7	-18.5	-12.7	9.5
Ibadan	Sum of two Gaussians	4.57	97.35	7.08	2.74	92.46	6.95	2.8			
	Sum of two Lorentzians	14.64	97.88	7.02	3.64	99.87	7.08	3.65			
	Sine wave	10.49	179.3	1.5	10.66	-	-	-			
	4th order Polynomial	5.78	14.27	4.87	-0.39	-0.01	-	-			
	Fourier on 4 Harmonics	a	b	c_1	c_2	c_3	c_4	d_1	d_2	d_3	d_4
		119.5	.57	-53.1	-65.4	-3.8	-30.7	-16.9	-15.0	-14.6	-4.2
Ikeja	Sum of two Gaussians	11.89	148.9	5.88	0.65	148.9	7.17	3.23			
	Sum of two Lorentzians	11.4	149.3	5.84	0.69	148.9	7.22	3.62			
	Sine wave	9.41	292.8	1.63	10.11	-	-	-			
	4th order Polynomial	11.4	26.52	1.13	-0.03	0.02	-	-			
	Fourier on 4 Harmonics	a	b	c_1	c_2	c_3	c_4	d_1	d_2	d_3	d_4
		135.0	.57	-74	-55.7	35.7	-20.1	-25.1	-37.1	-3.1	21.2
Ilorin	Sum of two Gaussians	4.33	107.9	6.03	2.42	107.6	8.47	1.84			
	Sum of two Lorentzians	5.86	108.2	6.06	2.61	106.5	8.73	1.67			
	Sine wave	10.72	192.7	1.47	10.95	-	-	-			
	4th order Polynomial	4.84	17.63	2.34	-0.02	-0.03	-	-			
	Fourier on 4 Harmonics	a	b	c_1	c_2	c_3	c_4	d_1	d_2	d_3	d_4
		107.1	.57	-52.2	-76.4	-4.1	-31.2	-27.7	-2.0	-9.0	9.4
Osogbo	Sum of two Gaussians	5.57	144.9	6.75	3.14	144.6	9.56	0.83			
	Sum of two Lorentzians	2.27	143.5	6.21	3.26	148.9	9.45	1.17			
	Sine wave	2.49	278.3	1.73	11.06	-	-	-			
	4th order Polynomial	3.82	25.24	-1.88	0.77	-0.06	-	-			
	Fourier on 4 Harmonics	a	b	c_1	c_2	c_3	c_4	d_1	d_2	d_3	d_4
		135.8	.57	-23.7	-80.0	24.5	-55.9	-33.0	-24.9	-17.5	5.8

Table 4. Statistical tests for solar Precipitable water and rainfall at all the stations

		PRECIPITABLE WATER					RAINFALL				
Location	Models	MBE	RMSE	MPE (%)	SE	R	MBE	RMSE	MPE (%)	SE	R
Abeokuta	Sum of two Gaussians	-0.08	0.03	-0.02	0.18	0.22	0.55	0.05	1.91	32.29	0.23
	Sum of two Lorentzians	-0.08	0.03	-0.02	0.18	0.22	0.55	0.05	1.91	35.59	0.23
	Fourier on fourth harmonics	0.00	0.00	0.00	0.05	1.00	0.00	0.00	0.00	0.17	0.99
	Sine wave	-1.21	4.17	-2.70	0.74	0.06	3.17	10.96	0.26	30.99	0.78
	4th order Polynomial	0.00	0.01	-0.46	0.63	0.25	-94.60	327.71	-7.86	33.24	0.24
Ado-Ekiti	Sum of two Gaussians	0.00	0.01	0.01	0.19	0.21	1.80	32.70	48.90	8.04	0.99
	Sum of two Lorentzians	0.00	0.01	0.01	0.24	0.21	0.00	5.30	0.20	8.11	0.99
	Fourier on four harmonics	0.00	0.00	0.00	0.09	1.00	0.00	4.60	0.00	9.09	0.99
	Sine wave	-1.20	4.16	-2.28	0.89	0.07	19.10	40.10	27.30	85.00	0.33
	4th order Polynomial	-2.78	9.64	5.28	0.78	0.29	-0.10	30.70	-9.10	35.60	0.84
Ibadan	Sum of two Gaussians	0.00	0.01	0.01	0.17	0.22	0.44	1.52	0.03	28.85	0.25
	Sum of two Lorentzians	0.00	0.01	0.01	0.15	0.22	0.44	1.52	0.03	35.02	0.25
	Fourier on four harmonics	0.00	0.00	0.00	0.05	1.00	0.00	0.00	0.00	5.07	1.00
	Sine wave	-1.21	4.18	-2.70	0.74	0.06	3.68	12.75	0.28	25.49	0.85
	4th order Polynomial	-0.45	1.55	-1.00	0.63	0.25	-102.4	354.53	-7.77	23.94	0.29
Ikeja	Sum of two Gaussians	-0.09	0.31	-0.18	0.33	0.03	0.11	0.39	0.01	28.93	0.23
	Sum of two Lorentzians	0.09	0.31	-0.18	0.31	0.03	0.11	0.29	0.01	3.99	0.23
	Fourier on four harmonics	0.00	0.00	0.00	0.17	0.99	0.00	0.00	0.00	9.02	0.99
	Sine wave	-1.31	4.52	-5.43	0.97	0.07	3.59	11.73	3.22	72.13	0.72
	4th order Polynomial	-1.59	5.52	3.33	0.95	0.28	-107.5	372.4	-7.1	49.7	0.2
Ilorin	Sum of two Gaussians	0.02	0.06	0.04	0.19	0.18	7.99	27.00	0.67	30.36	0.18
	Sum of two Lorentzians	0.02	0.06	0.04	0.27	0.18	7.99	27.00	0.67	27.70	0.18
	Fourier on four harmonics	0.00	0.00	0.00	0.11	1.00	0.00	0.00	0.00	3.24	0.99
	Sine wave	-0.87	0.14	-1.97	0.67	0.19	8.54	29.56	0.72	31.89	0.77
	4th order Polynomial	-5.95	20.63	-13.41	0.76	0.23	-92.51	320.45	-78.09	31.74	0.23
Osogbo	Sum of two Gaussians	0.00	0.01	0.00	0.15	0.22	0.39	1.36	0.03	39.93	0.24
	Sum of two Lorentzians	0.00	0.01	0.00	0.15	0.22	0.39	1.36	0.03	44.15	0.24
	Fourier on four harmonics	0.00	0.00	0.00	0.07	1.00	0.00	0.00	0.00	26.00	0.99
	Sine wave	-0.99	3.43	-2.05	0.64	0.35	5.28	18.30	0.35	1.77	0.58
	4th order polynomial	0.15	0.53	0.32	0.59	0.31	-113.7	394.01	-7.47	47.53	0.11

8. Conclusion

This study used five mathematical models to estimate rainfall and precipitable water distributions across six cities in the southwest of Nigeria. The values of the modelled data were compared with the values of the observed data. The accuracies of the models were evaluated using the performance indicators: mean bias error (MBE), root mean square error (RMSE), mean percentage error (MPE), correlation coefficient R, and standard error (SE). Generally, the fourth order polynomial model estimates had the poorest correlations with the observed data from the results of the performance indicators and the comparison between the observed and modelled data for both atmospheric variables at the selected locations. This observation implies that the polynomial model is not suitable for predicting these atmospheric variables in the selected locations. Similarly, the trend of the sine model failed to reveal the dual peaks of both rainfall and precipitable with their corresponding dips, particularly in the low-latitudes below Ilorin. The two-Gaussians and two-Lorentzians models had a better correlation with some of the variables than the duo of sine and polynomial models and, thus, may be considered for estimating the atmospheric variables. However, the Fourier model had the least values of the errors when compared with the other models. Also, the Fourier FH model reported the highest correlation coefficient values, R, of approximately 1.00 in all locations, indicating high accuracy in the estimated data. Thus, from the summary of the results, the Fourier model is recommended as the most suitable model for estimating rainfall and precipitable water in the selected locations.

References

Adefolalu, D., 1972. On the equivalent potential temperature of the tropical atmosphere and the "Little Dry Season" of West Africa. Niger. Meteor. Mag. 2, 15–40.

Adejokun, J., 1966. The Three-Dimensional Structure of The Inter-Tropical Discontinuity. Nigeria Met. Serv. Note 39.

Adejuwon, J., Odekunle, T., 2006. Variability and the Severity of the "Little Dry Season" in Southwestern Nigeria. Journal of Climate 19, 483–493. doi:https://doi.org/10.1175/JCLI3642.1.

Adekoya, J., 1979. Little Dry Season in Wet Africa. Msc thesis. Department of Meteorolgy, The Florida State University. USA.

Akinbobola, A., Okogbue, E.C., Ayansola, A.K., 2018. Statistical Modelling of Monthly Rainfall in Selected Stations in Forest and Savannah Eco-climatic Regions of Nigeria. J. Climatol. Weather Forecasting 6, 226. doi:https://doi.org/10.4172/2332-2594.1000226.

Balogun, E.E., 1981. Seasonal and spatial variations in thunderstorm activity over Nigeria. Weather 36, 192–197.

Dairo, O.F., Kolawole, L.B., 2018. Radio refractivity gradients in the lowest 100 m of the atmosphere over Lagos, Nigeria in the rainy-harmattan transition phase. Journal of Atmospheric and Solar-Terrestrial Physics 167, 169 – 176. doi:https://doi.org/10.1016/j.jastp.2017.12.001.

Ekwe, M., Joshua, J., Igwe, J., Osinowo, A., 2014. Mathematical Study of Monthly and Annual Rainfall Trends in Nasarawa State, Nigeria. IOSR Journal of Mathematics 10, 56–62.

Ilesanmi, O., 1981. Aspect of the precipitation climatology of the July-august rainfall minimum of southern Nigeria. N.G.A. Regional Planning Committee Seminar on Urban and Regional Problems in Nigeria, University of Ife, Ile-Ife, Nigeria 12.

Li, H., Fei, C., Wang, X., Ma, W., 2014. A Temperature-Based Model for Estimating Monthly Average Daily Global Solar Radiation in China. The Scientific World Journal 2014, 128754.

Maduekwe, A., Ogunmola, A., 1997. Estimation of the monthly average atmospheric Precipitable water vapour in Sokoto and its relationship with the horizontal global radiation. Nigerian Journal of Physics 9, 20–25.

Oduro-Afriye, K., 1992. Estimating precipitable water over West Africa from surface equivalent potential temperature and related potential instability indices. Atmospheric Research 28, 11–20.

Ogolo, E., Adeyemi, B., 2009. Variations and Trends of Some Meteorological Parameters at Ibadan, Nigeria. The Pacific Journal of Science and Technology 10, 981–987.

Ojo, O., 1970. The distribution of mean monthly precipitable water vapour and annual precipitation efficiency in Nigeria. Arch. Met. Geoph. Biokl. Serv. B 18, 221–238.

Omotosho, J., 1988. Spatial variation of rainfall in Nigeria during the Little Dry Season. Atmospheric Research 2, 137–147.

Ortiz de Galisteo, J., Cachorro, V., Toledano, C., Torres, B., Laulainen, N., Bennouna, Y., de Frutos, A., 2011. Diurnal cycle of precipitable water vapor over Spain. Q. J. Roy. Meteor. Soc. 137, 948–958. doi:https://doi.org/10.1002/qj.811.

Udoh, I., Okujagu, C., 2014. Distribution of mean annual precipitable water in Nigeria. Int. Journ. Sci. and Eng. 6, 174–176.

Willoughby, A.A., Aro, T.O., Owolabi, I.E., 2002. Seasonal variations of radio refractivity gradients in Nigeria. Journal of Atmospheric and Solar-Terrestrial Physics 64, 417–425.

Willoughbya, A.A., Ndubuisi, A.O., Dairo, O.F., Aizebeokhai, P.A., Oludotun, J.O., 2019. Performance analysis of temperature models for environmental monitoring in southwest nigeria. Nigerian Journal of Environment and Health 2, 20–29.